

Late sodium current and intracellular ionic homeostasis in acute ischemia

Carlotta Ronchi¹ · Eleonora Torre¹ · Riccardo Rizzetto¹ · Joyce Bernardi¹ · Marcella Rocchetti¹ · Antonio Zaza¹

Received: 5 July 2016 / Accepted: 3 January 2017 / Published online: 18 January 2017
© Springer-Verlag Berlin Heidelberg 2017

Abstract Blockade of the late Na^+ current (I_{NaL}) protects from ischemia/reperfusion damage; nevertheless, information on changes in I_{NaL} during acute ischemia and their effect on intracellular milieu is missing. I_{NaL} , cytosolic Na^+ and Ca^{2+} activities (Na_{cyt} , Ca_{cyt}) were measured in isolated rat ventricular myocytes during 7 min of simulated ischemia (ISC); in all the conditions tested, effects consistently exerted by ranolazine (RAN) and tetrodotoxin (TTX) were interpreted as due to I_{NaL} blockade. The results indicate that I_{NaL} was enhanced during ISC in spite of changes in action potential (AP) contour; I_{NaL} significantly contributed to Na_{cyt} rise, but only marginally to Ca_{cyt} rise. The impact of I_{NaL} on Ca_{cyt} was markedly enhanced by blockade of the sarcolemmal(s) $\text{Na}^+/\text{Ca}^{2+}$ exchanger (NCX) and was due to the presence of (Na^+ -sensitive) Ca^{2+} efflux through mitochondrial NCX (mNCX). sNCX blockade increased Ca_{cyt} and decreased Na_{cyt} , thus indicating that, throughout ISC, sNCX operated in the forward mode, in spite of the substantial Na_{cyt} increment. Thus, a robust Ca^{2+} source, other than sNCX and including mitochondria, contributed to Ca_{cyt} during ISC. Most, but not all, of RAN effects were shared by TTX. (1) The paradigm that attributes Ca_{cyt} accumulation during acute ischemia to decrease/reversal of sNCX transport may not be of general applicability; (2) I_{NaL} is enhanced during ISC, when the effect of Na_{cyt} on mitochondrial Ca^{2+} transport may

substantially contribute to I_{NaL} impact on Ca_{cyt} ; (3) RAN may act mostly, but not exclusively, through I_{NaL} blockade during ISC.

Keywords Acute ischemia · Late sodium current · Ranolazine · Na^+ homeostasis · Ca^{2+} homeostasis · Mitochondria

Introduction

Acute myocardial ischemia results in a characteristic pattern of metabolic and intracellular ion changes, ultimately leading to cytosolic Ca^{2+} (Ca_{cyt}) accumulation [5] and the resulting functional and structural derangements. Enhanced Na^+ influx, exceeding the functional reserve of the Na^+/K^+ pump, is widely considered as the “primum movens” of this process, being coupled to Ca_{cyt} homeostasis through changes in the equilibrium potential of the sarcolemmal $\text{Na}^+/\text{Ca}^{2+}$ exchanger (sNCX) (coupled exchanger theory) [9, 23, 28, 31].

Several mechanisms may account for enhanced a Na^+ influx during acute ischemia. While it is widely accepted that the Na^+/H^+ exchanger (NHE), driven by intracellular acidosis, may support large Na^+ influx upon reperfusion [19, 24, 47], there is disagreement about its role during ischemia [3, 32, 47]. Several studies show that blockade of a persistent component of Na^+ current (I_{NaL}), prevents Ca^{2+} overload and reduces injury following reperfusion [1, 7, 16, 45]. This suggests that I_{NaL} enhancement may contribute to increased Na^+ influx during the preceding ischemia. Exposure to ischemia components (i.e., H_2O_2 , hypoxia and ischemic metabolites) has indeed been shown to enhance I_{NaL} in standard V-clamp experiments [26, 40, 43, 46]. On the other hand, membrane

Electronic supplementary material The online version of this article (doi:10.1007/s00395-017-0602-9) contains supplementary material, which is available to authorized users.

✉ Antonio Zaza
antonio.zaza@unimib.it

¹ Department of Biotechnologies and Biosciences, University Milano-Bicocca, Piazza della Scienza 2, 20126 Milan, Italy

depolarization and shortening of action potential duration (APD), both correlates of acute ischemia, may reduce overall Na^+ current availability and time for I_{NaL} -mediated Na^+ influx, respectively. Therefore, whether I_{NaL} is actually enhanced during acute ischemia and contributes to cytosolic $\text{Na}^+/\text{Ca}^{2+}$ accumulation remains to be established. The present study aims to directly address these questions by measuring I_{NaL} and cytosolic ionic activities (Na_{cyt} and Ca_{cyt}) in isolated ventricular myocytes exposed to a simulated ischemia protocol.

The results obtained indicate that I_{NaL} was enhanced during simulated ischemia, in spite of the attending action potential (AP) changes, and significantly contributed to Na_{cyt} accumulation. However, the relationship between Na_{cyt} and Ca_{cyt} was more complex than predicted by the coupled exchanger theory, suggesting instead a role of ischemia-induced redistribution of Ca^{2+} between intracellular compartments, with mitochondria contributing as a Na_{cyt} -sensitive Ca^{2+} store.

Materials and methods

Cell isolation

Ventricular cardiomyocytes from male adult Sprague–Dawley rats (150–175 g) were isolated using a retrograde coronary perfusion method previously published with minor modifications [34]. Measurements were performed only in quiescent, rod-shaped, myocytes with clear striations. All experiments were approved and conducted accordingly to the guidelines stipulated by the Animal Care committee of University of Milano-Bicocca. The manuscript does not contain human data.

Simulated ischemia protocol

Cardiomyocytes were placed into a recording chamber and superfused at 36.5 °C with Tyrode's solution containing (mM): NaCl 154, KCl 4, CaCl_2 2, MgCl_2 1, HEPES 5, Glucose 5.5, adjusted to pH 7.3. Cells were paced at 1 Hz, either through the patch pipette or by field stimulation, throughout the protocol.

Ischemia was simulated by superfusing myocytes with a modified Tyrode's solution (ischemia mimic solution, ISC) containing (mM): NaCl 134, Na-lactate 20, KCl 8, CaCl_2 2, MgCl_2 1, HEPES 5, sucrose 37, adjusted to pH 6.8. Its composition reflects the major changes in the ischemic environment, as previously described by others [8, 10, 25, 30, 49].

ISC protocol has been performed here in normoxic condition, according to previous studies on ischemia [25] proving that the contribution of hypoxia to changes in

cardiomyocyte contractility is negligible; nevertheless, its absence should be considered in the interpretation of results (see “Discussion”).

The experimental protocol included pre-ISC stabilization in normal Tyrode's solution (about 2 min) followed by ISC superfusion for 7 min (Fig. S1). This ISC duration was selected in preliminary experiments as the maximal tolerated by the majority of cardiomyocytes; ISC wash-out (reperfusion) was almost invariably followed by contraction and death. In the following text, protocol phases are referred to as PRE (pre-ISC); 0.5ISC (0.5 min of ISC); 3ISC (3 min of ISC); 7ISC (7 min of ISC).

Cell shortening

Cardiomyocytes were field stimulated and the single-cell shortening was measured by video-edge detection system (Crescent electronics). The difference between maximal diastolic and systolic cell lengths was expressed as twitch amplitude, which was normalized within each cell to the value recorded in PRE conditions.

Electrophysiology

Myocytes were patch-clamped with borosilicate glass pipettes containing (mM): K^+ -aspartate 110, KCl 23, MgCl_2 3, HEPES KOH 5, EGTA KOH 0.5, GTP Na^+ -salt 0.4, ATP Na^+ -salt 5, creatine phosphate Na^+ -salt 5, CaCl_2 0.2 (calculated free- $\text{Ca}^{2+} = 10^{-7}$ M), adjusted to pH 7.2. Series resistance was <5 M Ω and was compensated to 80% of its value.

Action potentials (AP) were recorded (I -clamp with $I = 0$ pA) throughout the protocol. AP waveforms recorded in PRE condition and at 7ISC, respectively, were used as templates in AP-clamp experiments.

I_{NaL} was measured at PRE and 7ISC in AP-clamp mode as the current sensitive to 1 μM TTX [40]. To test whether ISC-induced changes in AP affected I_{NaL} magnitude during ISC, AP-clamp was applied with two modalities: (1) the AP templates recorded at PRE and 7ISC, which included ISC-induced changes, were applied during the corresponding phases of the protocol; (2) the AP template recorded at PRE, was applied at both PRE and 7ISC, thus disregarding ISC-induced changes. Differences between I_{NaL} recorded with the two AP-clamp modalities reflect the impact of ISC-induced membrane potential changes to I_{NaL} .

I_{NaL} magnitude during APs was quantified by integrating inward TTX-sensitive current from the beginning of repolarization to 90% of repolarization and dividing the result for the integration interval. This measurement, abbreviated in the following text and figures as “ I_{NaL} ”, reflects mean Na^+ influx rate during repolarization.

Currents were normalized to cell capacitance and expressed as current density (pA/pF).

Measurement of intracellular ionic activities

Na_{cyt} and Ca_{cyt} were measured in intact, field-stimulated (1 Hz) cardiomyocytes, loaded with Asante Natrium Green-2 (ANG-2) for Na^+ and FLUO4-AM for Ca^{2+} measurements, respectively. Cardiomyocytes were incubated with the membrane-permeant form of the dyes for 30 min, and then washed for 15 min. ANG-2 and FLUO4-AM emissions were collected through a 535 nm band pass filter, converted to voltage, low-pass filtered (200 Hz) and digitized at 2 kHz after further low-pass digital filtering (FFT, 100 Hz) and subtraction of background luminescence [2].

For Na^+ measurement, fluorescence recorded during ISC (F) was normalized to that recorded during the PRE phase (F_0) and expressed as F/F_0 . Considering that, Na_{cyt} changes were well within the range of linear dye response (Supplemental Figure S5), the uncalibrated Na^+ signal was considered adequate. Because dye response is slow relative to membrane potential changes, the Na^+ signal reflects an integrated value of Na_{cyt} during the whole electrical cycle.

Ca^{2+} fluorescence signal was calibrated by previously described methods [34], described in the Online Resource along with the potential bias introduced by intrinsic pH sensitivity of the dye. Since dye response is fast enough, the Ca^{2+} signal was evaluated as diastolic Ca^{2+} (Ca_D) and Ca^{2+} transient amplitude (Ca_T , i.e., difference between systolic Ca^{2+} and Ca_D). The sarcoplasmic reticulum (SR) Ca^{2+} content (Ca_{SR}) was estimated at 7ISC in separate subsets of cardiomyocytes, by applying an electronically timed 10 mM caffeine pulse. The caffeine solution was Ca^{2+} and Na^+ free, to prevent Ca^{2+} efflux through the sNCX. SR Ca^{2+} fractional release (Ca_{FR}) was obtained as the ratio between Ca_T at 7ISC and Ca_{SR} .

Pharmacological interventions

The contribution of different mechanisms to Na_{cyt} and Ca_{cyt} dynamics during ISC was evaluated by specific pharmacological interventions.

I_{NaL} contribution was tested by blocking the current with either ranolazine (RAN, 10 μM) or tetrodotoxin (TTX, 1 μM). Although at this concentration TTX can be safely considered to selectively block I_{NaL} [40], ancillary effects might be present for RAN. Therefore, whereas effects equally exerted by the two agents were considered to reflect I_{NaL} contribution, those peculiar of RAN may possibly result from ancillary effects of the drug. RAN and TTX were applied at the beginning of the PRE phase.

Contribution of sNCX and mNCX were tested by using the selective blockers SEA0400 (SEA, 1 μM) and

CGP37157 (CGP, 1 μM), respectively. Cariporide (CAR, 1 μM) and ouabain (OUAB, 1 mM) were used to inhibit the NHE and the Na^+/K^+ pump, respectively. RU360 (RU, 10 μM) was used to block the mitochondrial Ca^{2+} uniporter (MCU) [29], the main path of Ca^{2+} entry into mitochondria [21]. These agents were also added to the ISC solution; DMSO concentration was balanced in all the solutions.

Statistical analysis

The time courses of Na_{cyt} and Ca_{cyt} (Ca_T and Ca_D) during the protocol, shown in figures, were obtained by averaging records from N cells and are presented as mean \pm SE. Differences in twitch amplitude, Na_{cyt} and Ca_{cyt} were statistically evaluated at 0.5ISC, 3ISC, 7ISC (Supplemental figure S1). In the case of Na_{cyt} , peak value and the rate of rise ($d\text{Na}^+/\text{dt}$, by linear fitting of the rising phase) were also evaluated.

Differences between means were tested by paired T test or ANOVA as appropriate (Bonferroni's correction in post hoc comparisons). Statistical significance was defined as $p < 0.05$ (NS, not significant). Sample size is reported in each figure legend.

Results

Cell shortening and electrical activity

Twitch amplitude markedly decreased during early ISC (0.5ISC), to slowly recover to a stable level after 3 min (Fig. 1a). Twitch amplitude achieved a minimum at 0.5ISC ($-86.9 \pm 1.8\%$ of PRE; $p < 0.05$), recovered at 3ISC to $-12.4 \pm 18.5\%$ of PRE, without further changes at 7ISC ($-10.8 \pm 17.3\%$ of PRE) (Fig. 1b).

AP were elicited throughout ISC exposure (Fig. 1b), even when mechanical activity was almost absent. ISC partially depolarized diastolic potential (E_{diast}) and reduced dV/dt_{max} of phase 0 (Fig. 1c). APD at 90%, repolarization (APD90) prolonged up to 0.5ISC and then shortened (Fig. 1c). RAN treatment did not measurably affect AP response to ISC (Supplemental Figure S2).

Late Na^+ current

A small I_{NaL} was present during repolarization even in PRE conditions; this component was insensitive to blockade by RAN (Fig. 2). When the 7ISC AP template was applied at 7 min of ISC, I_{NaL} was increased by 77% ($p < 0.05$ vs PRE, Fig. 2b), a change completely prevented by RAN (Fig. 2b). When the PRE AP template was applied at 7ISC, I_{NaL} increment observed was, if anything, larger than seen

Fig. 1 Cell shortening and electrical activity during ISC. **a** Average traces \pm SE of contraction amplitude (left) and statistics at discrete time points during the protocol (arrows). **b** Representative traces of contraction (top) and action potentials (bottom) at discrete time points (arrows in a). **c** Statistics for diastolic membrane potential (E_{diast}), maximum depolarization rate (dV/dt_{max}) and action potential duration at 90% repolarization (APD90). CTRL $N = 8$. $^{\circ}p < 0.05$ vs PRE

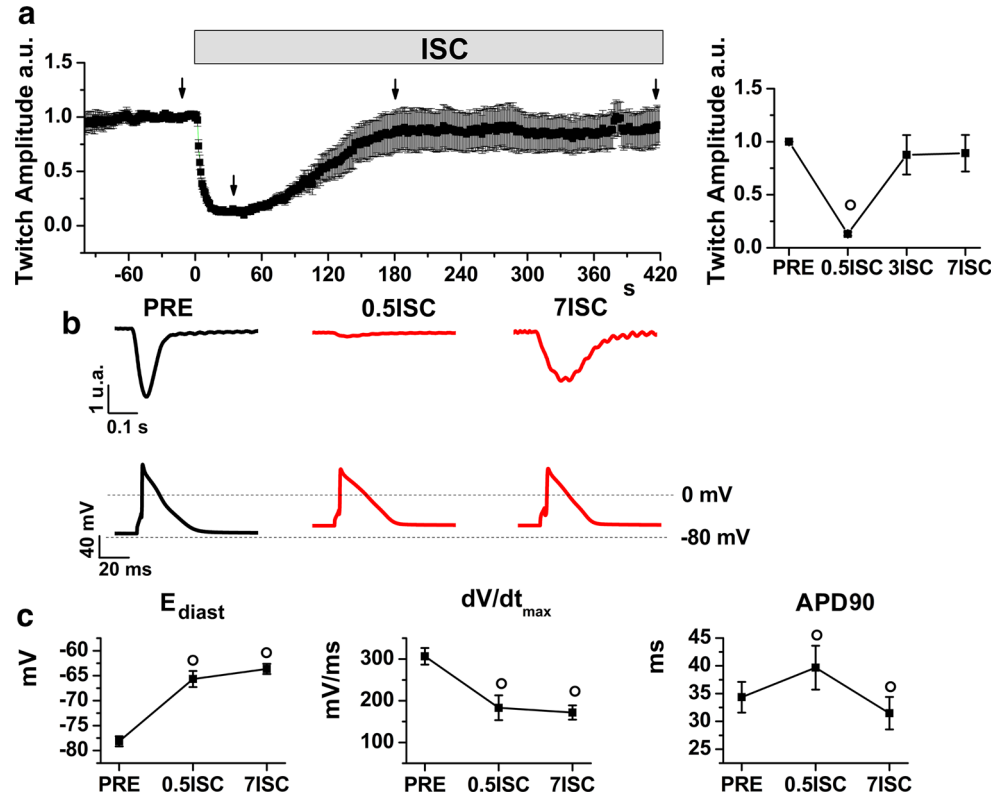
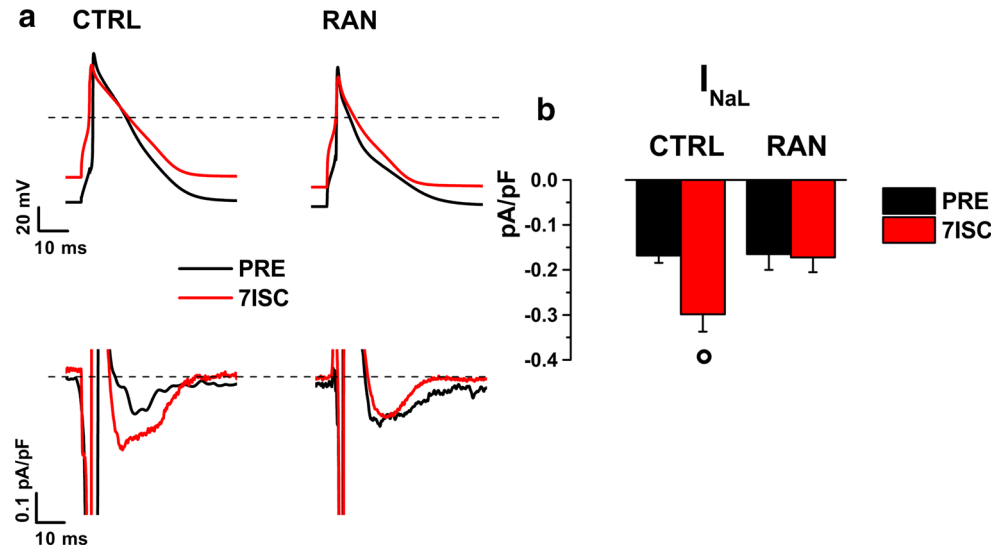


Fig. 2 Late Na^+ current (I_{NaL}) during ISC. **a** Representative action potentials templates (top) and the respective TTX-sensitive currents (bottom) at PRE (black line) and 7ISC (red line) time points in CTRL and RAN groups. **b** Statistics for I_{NaL} at PRE and 7ISC. $N > 6$ for both groups. $^{\circ}p < 0.05$ vs PRE



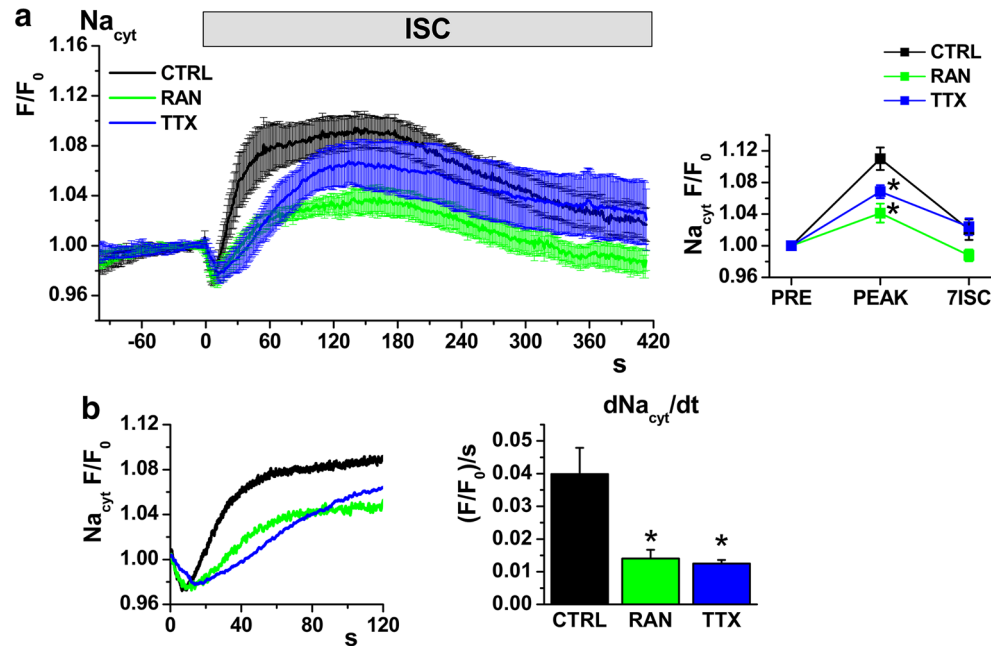
with the previous protocol (88%, $p < 0.05$ vs PRE, Supplemental Figure S3). Thus, I_{NaL} may significantly increase during ISC in spite of the attending membrane potential changes, which, as expected, reduced overall I_{Na} availability (reduced dV/dt_{max} , see above).

Cytosolic Na^+

Changes in Na_{cyt} during ISC were assessed in intact, field-stimulated (1 Hz) cardiomyocytes in the absence (CTRL)

and presence of I_{NaL} blockade by either RAN or TTX. After an initial dip, Na_{cyt} increased during ISC, reaching a peak at about 1–2 min, and then slowly declined (Fig. 3a). RAN and TTX significantly reduced peak Na_{cyt} (Fig. 3a) and the rate of Na_{cyt} increment (Fig. 3b); the effect was similar between the two agents. This suggests that I_{NaL} enhancement significantly contributed to, but was not the only factor, in Na_{cyt} accumulation during ISC. When both I_{NaL} and NHE were blocked simultaneously (CAR + TTX), ISC failed to induce Na_{cyt} accumulation

Fig. 3 Effect of I_{NaL} blockade (RAN, TTX) on cytosolic Na^+ (Na_{cyt}) during ISC. **a** Average traces \pm SE of Na_{cyt} during the ISC protocol in CTRL, RAN and TTX treatment groups; statistics of Na_{cyt} changes (normalized to values at PRE) at peak Na_{cyt} and at 7ISC time points. **b** Average Na_{cyt} traces (as in a) during the early ISC phase to illustrate differences in Na_{cyt} accumulation rate; statistics for Na_{cyt} accumulation rate (dNa_{cyt}/dt). CTRL $N = 14$; RAN $N = 9$; TTX $N = 12$. * $p < 0.05$ vs CTRL



(Supplemental Figure S4), thus pointing to NHE as the other Na^+ influx route [35].

To test whether the Na^+/K^+ pump remained functional during ISC and contributed to the late Na_{cyt} decline, cardiomyocytes were exposed to ISC in the presence of ouabain (OUAB). Under this condition, Na_{cyt} monotonically increased throughout ISC superfusion (Supplemental Figure S5), indicating that in the present settings, the Na^+/K^+ pump was active and contributed to limit Na_{cyt} accumulation.

Cytosolic Ca^{2+}

Changes in Ca_{cyt} during ISC were assessed in intact, field-stimulated (1 Hz) cardiomyocytes (Fig. 4). Both Ca_D and Ca_T increased during ISC; at variance with Na_{cyt} , the increment was not preceded by a dip. Ca_D monotonically increased to achieve a more or less stable level at 3 min (Fig. 4a). Ca_T increment followed a sigmoidal time course, thus lagging behind Ca_D ; it achieved a peak at about 3 min and then slowly declined (Fig. 4a). RAN slightly, but significantly, decreased Ca_D and visibly minimized its variability across cells, an effect not shared with TTX (Fig. 4a). The same was true for Ca_T even if, probably because of its larger variability, RAN effect on this parameter did not achieve significance (Fig. 4a). Both RAN and TTX tended to decrease Ca_{SR} , but when analyzed separately for each I_{NaL} blocker their effect did not achieve statistical significance (Fig. 4b). However, when the data from RAN and TTX groups were pooled, I_{NaL} blockade significantly reduced Ca_{SR} at 7ISC (80.7 ± 8.5 vs 60.8 ± 4.7 μM ; $p < 0.05$, Fig. 4b). Ca_{FR} was not affected by I_{NaL} blockade (Fig. 4b).

These observations are consistent with the common notion that Ca_{cyt} increases during acute ischemia; however, neither its timing with respect to Na_{cyt} , nor its unexpected insensitivity to I_{NaL} blockade, were consistent with its dependency on enhanced Na^+ influx. The (small) effect of RAN on Ca_D , not shared by TTX, might reflect an agent-specific ancillary action.

The unexpected lack of Ca_{cyt} response to reduced Na^+ influx, led us to question sNCX role in mediating Ca_{cyt} accumulation during ISC. To address this point, Ca_{cyt} measurements were repeated in the presence of sNCX blockade.

Role of the sarcolemmal Na^+/Ca^{2+} exchanger

To assess the role of sNCX during ISC, its specific inhibitor SEA [42] was also added to the ISC solution (ISC + SEA, Fig. 5).

In the presence of SEA, ISC-induced Na_{cyt} accumulation was reduced and Ca_{cyt} accumulation (Ca_D , Ca_T , Ca_{SR}) was markedly enhanced (Supplemental Figure S6). The direction of the reciprocal changes in Na_{cyt} and Ca_{cyt} unequivocally indicates that, during ISC, sNCX still operated in its forward mode, thus supporting Ca^{2+} efflux, rather than influx. Notably, forward sNCX operation persisted in spite of the attending increase in Na_{cyt} ; moreover, the Ca_{cyt} increment induced by ISC in the presence of sNCX blockade (SEA group) was twice as large as that observed during SEA alone (Supplemental Figure S7). These findings indicate that large, sNCX-independent, Ca^{2+} sources contribute to Ca_{cyt} build up during ISC.

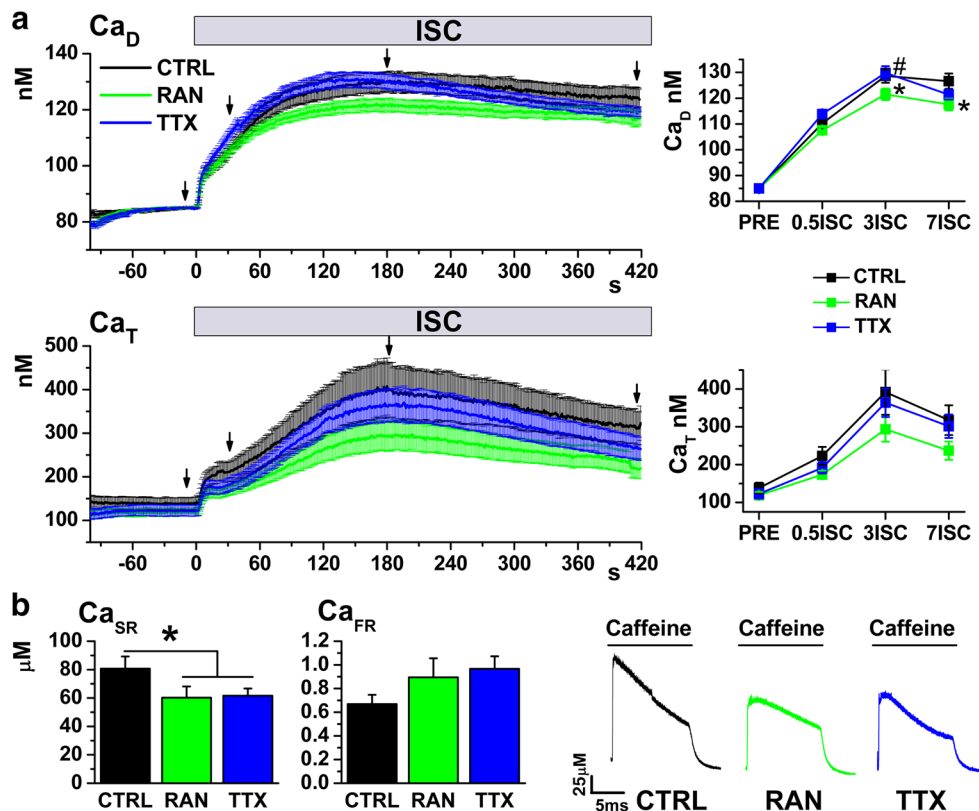


Fig. 4 Effect of I_{NaL} blockade (RAN, TTX) on cytosolic Ca^{2+} (Ca_{cyt}) during ISC. **a** Average traces \pm SE of diastolic Ca^{2+} (Ca_D) and Ca^{2+} transient amplitude (Ca_T) during the ISC protocol in CTRL, RAN and TTX treatment groups; statistics of Ca_{cyt} at discrete time points (arrows) during the protocol (CTRL $N = 22$; RAN $N = 19$;

TTX $N = 19$). **b** Statistics for SR Ca^{2+} content (Ca_{SR}) and SR Ca^{2+} fractional release (Ca_{FR}) at protocol end (CTRL $N = 19$; RAN $N = 13$; TTX $N = 10$); representative Ca^{2+} transient triggered by caffeine in each group. * $p < 0.05$ vs CTRL; # $p < 0.05$ vs RAN

Notably, during ISC + SEA, both RAN (+RAN) and TTX (+TTX) significantly reduced Ca_{cyt} accumulation (Fig. 5a), with their effect being substantially larger than during ISC alone (Fig. 4). This suggests the contribution to Ca_{cyt} accumulation of a Na^+ -sensitive Ca^{2+} source, whose role was unveiled by sNCX blockade.

Consistent with the increase in overall cell Ca^{2+} content expected from sNCX blockade, Ca_{SR} at 7ISC was higher in ISC + SEA (SEA) than in ISC alone (CTRL) (116.7 ± 11.6 vs 80.7 ± 8.5 μM ; $p < 0.05$; Supplemental Figure S6a). RAN slightly but significantly reduced Ca_{SR} even in the presence of SEA (Fig. 5b), thus suggesting its ability to modulate Ca_{cyt} independently of sNCX. This effect did not achieve significance with TTX, which, in this respect, was less efficient than RAN. Ca_{FR} was unchanged by either RAN or TTX (Fig. 5b) thus arguing against modulation of ryanodine receptors (RyRs) as a major player in the effects exerted by the two agents.

The significant effect of I_{NaL} blockade on Ca_{cyt} in Fig. 5 suggests that, at least under sNCX inhibition, a Na_{cyt} -sensitive intracellular compartment may contribute to its accumulation during ISC. Mitochondria are an intracellular Ca^{2+} compartment, potentially affected by ISC and

endowed of Na_{cyt} -sensitive Ca^{2+} transport. The latter is represented by mNCX, which may either uptake or release Ca^{2+} from mitochondria depending on the electrochemical gradient for the transport. To test this hypothesis, the experiments were repeated in the presence of mNCX blockade.

Role of the mitochondrial Na^+/Ca^{2+} exchanger

mNCX was selectively blocked by CGP [12], which was added to the ISC solution either alone, or in the presence of SEA.

When applied alone (CGP group, Fig. 6 left), CGP did not measurably affect Ca_{cyt} accumulation during ISC (Fig. 6a); however, it significantly increased Ca_{SR} (Fig. 6b), thus suggesting a shift of Ca^{2+} from the mitochondrial to the SR compartment. On the other hand, when CGP was applied in the presence of SEA (+CGP group; Fig. 6 right), Ca_{cyt} accumulation and Ca_{SR} were significantly reduced. Thus, at least in the presence of the high Ca_{cyt} levels achieved under sNCX blockade, mitochondria provided a Ca^{2+} source, with mNCX supporting Ca^{2+} efflux to the cytosol [27]. Ca_{FR} was not affected by CGP

Fig. 5 Effect of I_{NaL} blockade (RAN, TTX) on cytosolic Ca^{2+} during ISC in the presence of sNCX blockade (SEA).

a Average traces \pm SE of diastolic Ca^{2+} (Ca_D) and Ca^{2+} transient amplitude (Ca_T) during the ISC protocol in CTRL, RAN and TTX treatment groups; statistics of Ca_{cyt} at discrete time points (arrows) during the protocol; statistics of Ca_{cyt} at discrete time points (arrows) during the protocol (SEA $N = 23$; SEA + RAN $N = 20$; SEA + TTX $N = 18$).
b Statistics for SR Ca^{2+} content (Ca_{SR}) and SR Ca^{2+} fractional release (Ca_{FR}) at protocol end (SEA $N = 9$; SEA + RAN $N = 9$; SEA + TTX $N = 9$); representative Ca^{2+} transient triggered by caffeine superfusion in each group.
 $^{\S}p < 0.05$ vs SEA

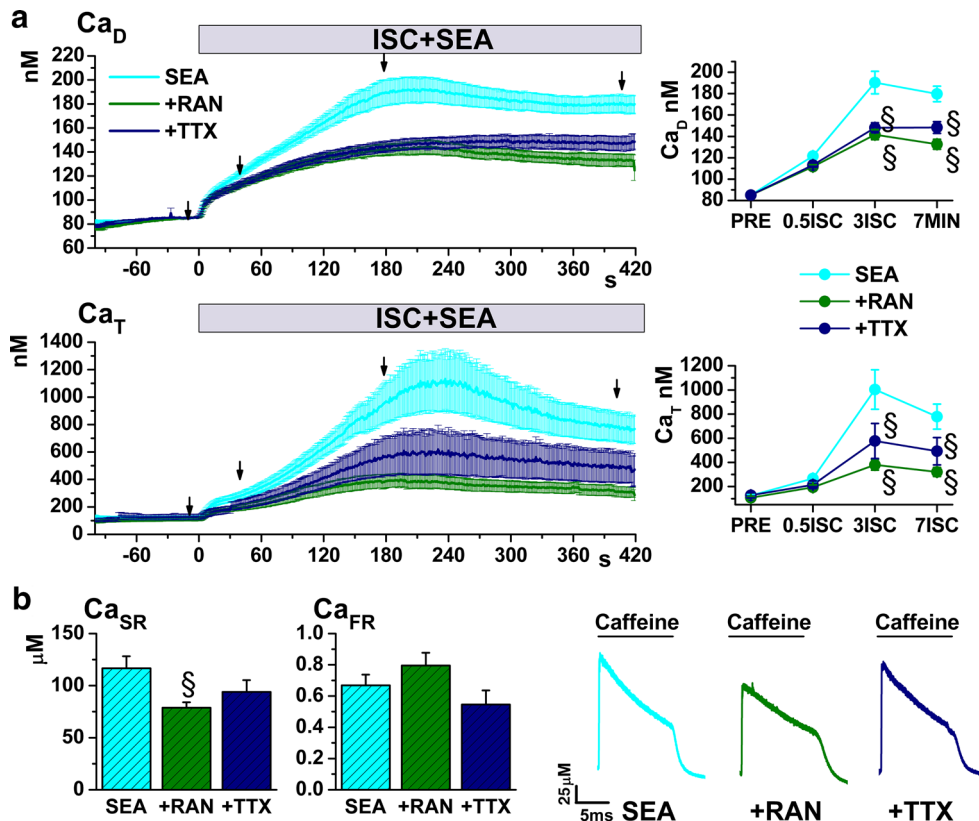
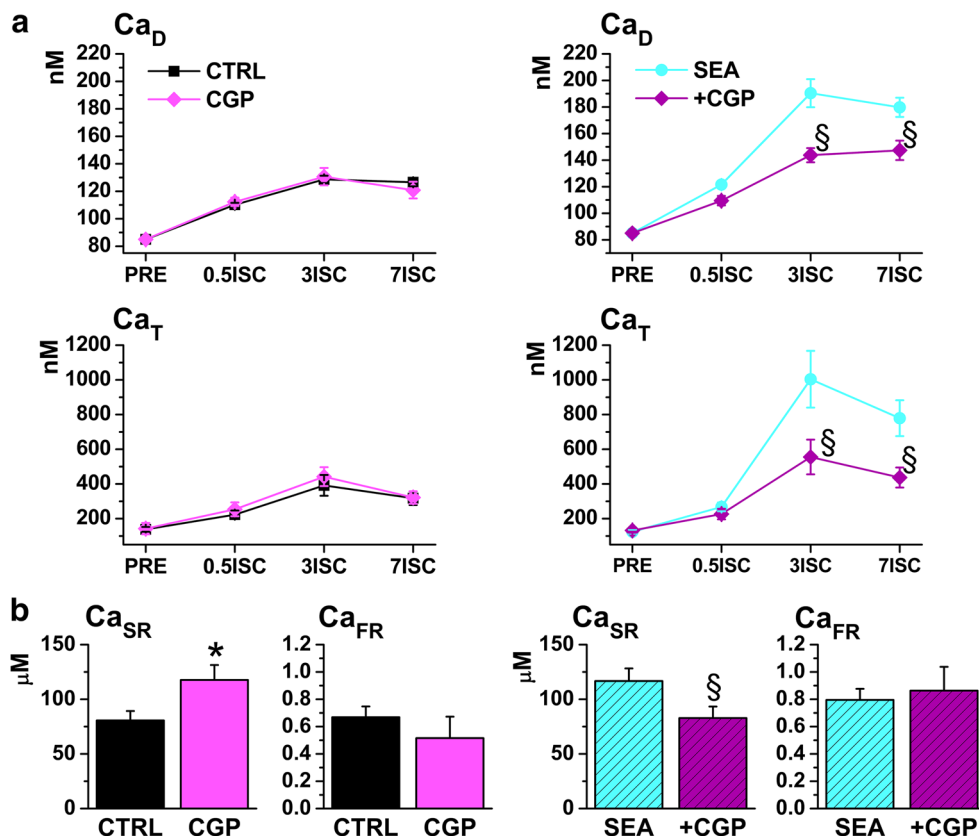


Fig. 6 Effect of mNCX blockade (CGP) on Ca_{cyt} and Ca_{SR} during ISC. *Left* effect of CGP alone; *right* effect of CGP in the presence of SEA.

a Statistics for diastolic Ca^{2+} (Ca_D , top) and Ca^{2+} transient amplitude (Ca_T , bottom) at discrete protocol time points (CTRL $N = 22$; CGP $N = 8$; SEA $N = 23$; SEA + CGP $N = 16$); **b** statistics for SR Ca^{2+} content (Ca_{SR}) and SR fractional release (Ca_{FR}) at the end of protocol (CTRL $N = 19$; CGP $N = 8$; SEA $N = 10$; SEA + CGP $N = 14$).
 $^*p < 0.05$ vs CTRL, $^{\S}p < 0.05$ vs SEA



(Fig. 6b), again arguing against the involvement of RyRs modulation in the observed effects.

In the presence of sNCX blockade, the effects of CGP, RAN and TTX on Ca_{cyt} accumulation during ISC were strikingly similar (Supplemental Figure S8). This supports the view that I_{NaL} blockade may limit Ca_{cyt} accumulation by reducing Na_{cyt} availability to fuel mNCX-mediated Ca^{2+} efflux from mitochondria.

To further test the role of mitochondria as a Ca^{2+} source during ISC, MCU was selectively blocked by RU [29] in the presence of sNCX blockade (+RU). RU reduced Ca_{cyt} accumulation, achieving statistical significance for Ca_D (Fig. 7a). In the presence of SEA + RU, CGP failed to modify Ca_{cyt} (Supplement Figure S10). These observations confirm a role of mitochondria in Ca_{cyt} increment during ISC and support the view that the effect of CGP on Ca_{cyt} (Fig. 6 right) were due to inhibition of mitochondrial Ca^{2+} efflux. RU also increased Ca_{SR} (Fig. 7b) likely reflecting transfer of Ca^{2+} from the mitochondrial compartment to the SR one.

Discussion

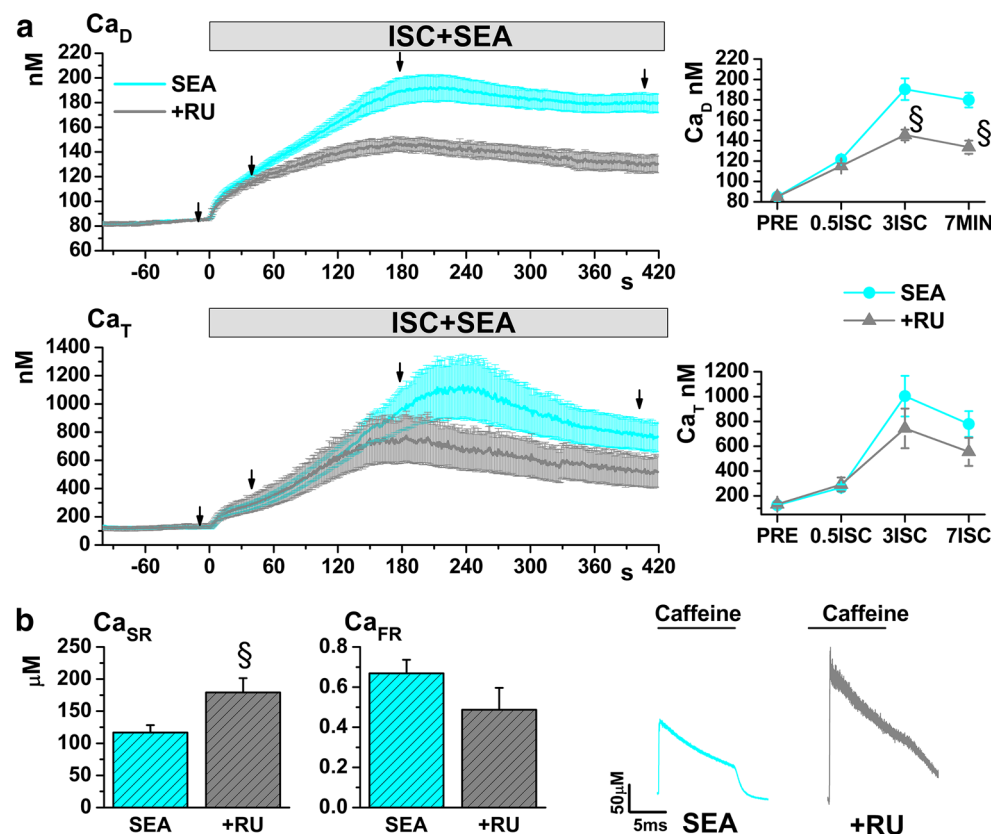
The main findings of this study are that during ISC: (1) I_{NaL} was increased in spite of AP changes; (2) I_{NaL} blockade reduced Na_{cyt} accumulation, but failed to affect Ca_{cyt}

accumulation unless sNCX was blocked; (3) sNCX contributed to Ca_{cyt} clearance (as opposed to accumulation) throughout ISC; (4) blockade of I_{NaL} and mNCX exerted similar effects on ISC-induced Ca_{cyt} accumulation, at least under conditions of substantial Ca^{2+} overload.

Relevance of ISC as a model of acute myocardial ischemia

Tissue response to acute ischemia is highly dynamic and closely dependent on a number of conditions; thus, any experimental model of acute ischemia is necessarily specific and unlikely to be of general applicability. Furthermore, an isolated myocyte, oxygenated through aqueous superfusion (low O_2 solubility) and contracting without external load, cannot be strictly compared to in vivo ischemia. Nevertheless, information of general relevance on the mechanisms that can contribute to ischemic damage, can still be acquired by observing the response to conditions known to occur during it. The ischemic condition adopted in this study (ISC), although encompassing the major factors present in tissue ischemia, differs from it for the absence of hypoxia. Although hypoxia was shown to have little role in the contractile pattern during ISC application [25], it might affect the mechanisms by which such a pattern is achieved in a given time-frame. For

Fig. 7 Effect of MCU blockade (RU) on cytosolic Ca^{2+} during ISC (in the presence of sNCX blockade). **a** Average traces \pm SE of diastolic Ca^{2+} (Ca_D) and Ca^{2+} transient amplitude (Ca_T) during ISC + SEA alone (SEA) and in the presence of MCU blockade (+RU); Ca_D and Ca_T statistics at discrete time points; **b** statistics for SR Ca^{2+} content (Ca_{SR}) and SR Ca^{2+} fractional release (Ca_{FR}) at protocol end; representative caffeine-induced Ca^{2+} transients. SEA $N = 9$; +RU $N = 10$. $^{\S}p < 0.05$ vs SEA



instance, hypoxia would likely accelerate ATP decay and reactive oxide species (ROS) production, both factors known to accelerate Na_{cyt} accumulation and facilitate reversal of sNCX transport. Therefore, failure of sNCX to switch to the reverse mode, and the modest effect of I_{NaL} blockade, might be model-specific. However, the contribution of sNCX-independent Ca^{2+} sources (including mitochondria) to Ca_{cyt} accumulation in the presence of factors certainly present during real ischemia, may have general relevance. A further factor to be considered is that, whereas generated within the myocyte under true ischemia, lactic acid was applied extracellularly. This might reduce NHE contribution to Na^+ loading, which was nonetheless substantial (Supplemental Figure S4).

To mimic what is reported to occur during ischemia, the ISC solution was slightly hyperosmolar [25]. The possibility that this accounted for the observed changes in the intracellular milieu was ruled out in preliminary experiments (Supplemental Figure S9).

Because of the above features, ISC reproduces conditions closer to those of a “border zone”, not directly ischemic (still energetically competent) but exposed to factors released by the neighboring ischemic area [11].

ISC-induced I_{NaL} enhancement

A link between I_{NaL} enhancement and ischemia/reperfusion injury has been firmly established by previous studies [1, 4, 7, 39, 50]. However, considering the opposing effect of ISC-induced membrane potential changes, I_{NaL} enhancement by ISC was far from predictable.

Contribution of I_{NaL} and Na^+/H^+ exchanger to cytosolic Na^+ accumulation

About 50% of ISC-induced Na_{cyt} accumulation was similarly prevented by RAN and TTX. Being shared by both agents, this effect is likely to result from I_{NaL} blockade. When NHE was also blocked (Supplemental Figure S4), ISC-induced Na_{cyt} accumulation was completely abolished; this suggests that Na^+ influx via NHE accounted for the remaining 50% (this quantitative estimate does not take into account potential interactions between the two transports). Although the presence in ISC of lactic acid likely afforded relatively fast H^+ equilibration across the membrane, acidosis was primarily extracellular in the present setting; this might explain the initial dip in Na_{cyt} time course (Fig. 3). The present findings suggest that, under the present experimental conditions, NHE was still active during ISC. The monotonic increase in Na_{cyt} during exposure to ouabain (Supplemental Figure S5) indicates that I_{NaL} - and NHE-mediated Na^+ influx were in balance with Na^+ extrusion through the Na^+/K^+ pump, which

remained active throughout the ISC period and was responsible for the late decay in Na_{cyt} .

I_{NaL} contribution to cytosolic Ca^{2+} accumulation

In spite of its remarkable effect on Na_{cyt} , I_{NaL} blockade unexpectedly failed to affect ISC-induced Ca_{cyt} accumulation (Fig. 4). This might simply reflect inadequacy of the I_{NaL} -dependent Na_{cyt} perturbation in overriding Ca_{cyt} homeostatic control; indeed, I_{NaL} blockade tended to reduce Ca_{SR} , potentially revealing a role for SR in buffering I_{NaL} -induced perturbation. However, the observation that the effect of I_{NaL} blockade was unmasked by sNCX blockade implies that a Ca^{2+} source independent of sNCX, and at least partially sensitive to I_{NaL} blockade (or Na_{cyt}), must have contributed to ISC-induced Ca_{cyt} accumulation.

sNCX is often claimed to work in reverse mode during ischemia [43, 48], thereby providing a direct path for Ca^{2+} influx. This was clearly not the case in the present setting; however, sNCX mode may depend on the duration and extent of ischemia. Nevertheless, changes in Na_{cyt} compatible with forward sNCX operation have been reported after sNCX knock-out in intact murine hearts subjected to no-flow ischemia (Fig. 5 in Ref. [18]).

Mitochondrial contribution to cytosolic Ca^{2+} accumulation

Mitochondria represent a significant Ca^{2+} compartment, physiologically uptaking Ca^{2+} through MCU [21] and extruding it to cytosol through mNCX, a Na_{cyt} -sensitive transport [6, 27].

CGP effect in the absence of SEA suggests that, under basal conditions, mNCX blockade may promote a shift of Ca^{2+} from mitochondria to the SR. This implies that, during ISC, mitochondria contribute to buffer Ca_{cyt} through mNCX-mediated Ca^{2+} uptake. In the present setting, the impact of I_{NaL} blockade on mitochondrial buffering was probably small enough not to affect Ca_{cyt} .

On the other hand, when sNCX was blocked, CGP reduced ISC-induced Ca_{cyt} accumulation, thus supporting the view that sizable mNCX-mediated Ca^{2+} efflux from mitochondria may occur during ISC in the presence of substantial Ca^{2+} overload [6, 37, 44]. Because mNCX flux is Na_{cyt} -dependent, this might account for the I_{NaL} -sensitive component of Ca_{cyt} accumulation observed under sNCX blockade.

At the conditions used in the present experiments, RU is a selective blocker of MCU, without effect on I_{CaL} or SR Ca^{2+} uptake/release [29, 36]. Functional exclusion of the mitochondrial compartment by MCU blockade caused a shift of Ca^{2+} to the SR, reduced Ca_{cyt} accumulation and

abolished the effect of mNCX blockade. Concomitance of reduced Ca_{cyt} with increased Ca_{SR} is consistent with micro-domain communication between mitochondria and SR [22].

To summarize, sNCX blockade seemingly changed the role of mitochondria during ISC from Ca^{2+} sink to Ca^{2+} source; the simplest way to explain this effect is the rather dramatic increase in overall cell Ca^{2+} content present in this condition, possibly reducing mitochondrial and SR Ca^{2+} buffering reserves. We surmise that such a Ca^{2+} overload might be achieved, even in the absence of sNCX blockade, during in vivo cardiac ischemia. Therefore, the specific effect of mNCX inhibition might depend on the duration and extent of ischemia; nevertheless, the contribution of mitochondria as a further Na_{cyt} -sensitive compartment contributing to Ca_{cyt} changes may be regarded as an observation of general value.

Additional potential sources of cytosolic Ca^{2+} accumulation

As a Na_{cyt} -sensitive Ca^{2+} compartment, mitochondria are of particular relevance to changes caused by I_{NaL} enhancement. Nonetheless, they are unlikely to fully account for the large source of Ca_{cyt} required to support forward sNCX operation during ISC, in spite of the attending increase in Na_{cyt} and membrane depolarization (both favoring sNCX reversal).

Because voltage-gated Ca^{2+} channels are potently inhibited by acidosis [20, 38] I_{CaL} is unlikely to be enhanced during ISC; however, a H^+ -gated background Ca^{2+} conductance (TRPA1) [17] is expressed in the heart and shown to contribute to ischemia/reperfusion damage [33].

Protons compete with Ca^{2+} for binding to intracellular buffers, troponin C in particular [15, 41]. In the present setting, this is suggested by the virtual absence of contraction during early ISC, occurring in spite of persisting Ca^{2+} transients. Therefore, acidosis might support substantial release of free Ca^{2+} to the cytosol through a mechanism independent of transmembrane fluxes. Because sarcolemmal Na^+ gradient is crucial for intracellular H^+ clearance through NHE, this Ca^{2+} source may also be modulated, albeit indirectly, by I_{NaL} blockade.

Discrepancy between TTX and RAN effects

RAN and TTX shared the majority of effects during ISC exposure, supporting their origin from I_{NaL} inhibition. However, unlike TTX, RAN reduced Ca_{D} during ISC under baseline condition and limited Ca_{SR} increment during SEA exposure. This points to modulation by RAN of a Ca^{2+} compartment insensitive to TTX. RAN has been

shown to stabilize membrane potential of mitochondria during ischemia [1, 13, 14, 51], which would enhance their ability to retain Ca^{2+} . However, this has been attributed to limitation of Na_{cyt} accumulation, an effect that should be shared by TTX. The possibility that RAN may affect mitochondrial performance as a Ca^{2+} compartment also independently of I_{NaL} blockade may deserve further investigation.

Conclusions

Some of the observed effects of ISC may be model-specific (i.e., depend on the duration and extent of the ischemic condition) and, as such, of restricted applicability. These may include poor sensitivity of Ca_{cyt} to I_{NaL} blockade and persistence of forward sNCX operation. Nevertheless, other observations lead to conclusions likely of more general relevance: (1) I_{NaL} can be enhanced during acute ischemia, irrespective of membrane potential changes, and significantly contribute to Na_{cyt} accumulation; (2) Ca^{2+} sources other than sNCX substantially contribute to Ca_{cyt} increment and, at least in the early phase of acute ischemia, may oppose reversal of sNCX flux; (3) under conditions of Ca^{2+} overload, mitochondria may act as a Na_{cyt} -sensitive Ca_{cyt} source, thus providing a mechanism, beyond sNCX modulation, to account for I_{NaL} -induced perturbation of intracellular milieu. A further conclusion is that most, but not all, RAN effects on intracellular milieu may result from I_{NaL} blockade.

Acknowledgements This research was supported by grant from Gilead Inc. (Fremont, CA, US) and FAR 2015 to A. Zaza. We are grateful to Dr. Luiz Belardinelli for providing stimulating discussion throughout the execution of the study and Dr. Luca Sala for contributing to some experiments and providing insightful comments on the manuscript.

Compliance with ethical standards

All experiment were approved and conducted in accordance with guidelines issued by the Animal Care Committee of the University Milano-Bicocca, in compliance with the ethical standards laid down in the 1964 Declaration of Helsinki and its later amendments. The manuscript does not contain human data.

Conflict of interest The study has been partially funded by Gilead, Inc. (Fremont, CA), which is the patent holder for Ranolazine. The authors declare that they have no further conflict of interest.

References

1. Aldakkak M, Camara AK, Heisner JS, Yang M, Stowe DF (2011) Ranolazine reduces Ca^{2+} overload and oxidative stress and improves mitochondrial integrity to protect against ischemia

- reperfusion injury in isolated hearts. *Pharmacol Res* 64:381–392. doi:10.1016/j.phrs.2011.06.018
2. Alemanni M, Rocchetti M, Re D, Zaza A (2011) Role and mechanism of subcellular Ca²⁺ distribution in the action of two inotropic agents with different toxicity. *J Mol Cell Cardiol* 50:910–918. doi:10.1016/j.yjmcc.2011.02.008
 3. Allen DG, Xiao XH (2003) Role of the cardiac Na⁺/H⁺ exchanger during ischemia and reperfusion. *Cardiovasc Res* 57:934–941. doi:10.1016/s0008-6363(02)00836-2
 4. Belardinelli L, Shryock JC, Fraser H (2006) Inhibition of the late sodium current as a potential cardioprotective principle: effects of the late sodium current inhibitor ranolazine. *Heart* 92(Suppl 4):iv6–iv14. doi:10.1136/hrt.2005.078790
 5. Bernink FJ, Timmers L, Beek AM, Diamant M, Roos ST, van Rossum AC, Appelman Y (2014) Progression in attenuating myocardial reperfusion injury: an overview. *Int J Cardiol* 170:261–269. doi:10.1016/j.ijcard.2013.11.007
 6. Boyman L, Williams GS, Khananshvil D, Sekler I, Lederer WJ (2013) NCLX: the mitochondrial sodium calcium exchanger. *J Mol Cell Cardiol* 59:205–213. doi:10.1016/j.yjmcc.2013.03.012
 7. Calderon-Sanchez EM, Dominguez-Rodriguez A, Lopez-Haldon J, Jimenez-Navarro MF, Gomez AM, Smani T, Ordonez A (2016) Cardioprotective effect of ranolazine in the process of ischemia-reperfusion in adult rat cardiomyocytes. *Rev Esp Cardiol (Engl Ed)* 69:45–53. doi:10.1016/j.rec.2015.02.027
 8. Caldwell JC, Burton FL, Cobbe SM, Smith GL (2012) Amplitude changes during ventricular fibrillation: a mechanistic insight. *Front Physiol* 3(147):1–8. doi:10.3389/fphys.2012.00147
 9. Chen S, Li S (2012) The Na⁺/Ca²⁺ exchanger in cardiac ischemia/reperfusion injury. *Med Sci Monit* 18:RA161–RA165. doi:10.12659/MSM.883533
 10. Cordeiro JM, Howlett SE, Ferrier GR (1994) Simulated ischemia and reperfusion in isolated guinea pig ventricular myocytes. *Cardiovasc Res* 28:1794–1802. doi:10.1093/cvr/28.12.1794
 11. Coronel R, Wilms-Schopman FJ, Fiolet JW, Opthof T, Janse MJ (1995) The relation between extracellular potassium concentration and pH in the border zone during regional ischemia in isolated porcine hearts. *J Mol Cell Cardiol* 27:2069–2073. doi:10.1016/0022-2828(95)90028-4
 12. Cox DA, Conforti L, Sperelakis N, Matlib MA (1993) Selectivity of inhibition of Na⁺–Ca²⁺ exchange of heart mitochondria by benzothiazepine CGP-37157. *J Cardiovasc Pharmacol* 21:595–599. doi:10.1097/00005344-199304000-00013
 13. Dehina L, Descotes J, Chevalier P, Bui-Xuan B, Romestaing C, Dizerens N, Mamou Z, Timour Q (2014) Protective effects of ranolazine and propranolol, alone or combined, on the structural and functional alterations of cardiomyocyte mitochondria in a pig model of ischemia/reperfusion. *Fundam Clin Pharmacol* 28:257–267. doi:10.1111/fcp.12033
 14. Gadicherla AK, Stowe DF, Antholine WE, Yang M, Camara AK (2012) Damage to mitochondrial complex I during cardiac ischemia reperfusion injury is reduced indirectly by anti-anginal drug ranolazine. *Biochim Biophys Acta* 1817:419–429. doi:10.1016/j.bbabi.2011.11.021
 15. Garciaarena CD, Youm JB, Swietach P, Vaughan-Jones RD (2013) H⁺-activated Na⁺ influx in the ventricular myocyte couples Ca²⁺(+)-signalling to intracellular pH. *J Mol Cell Cardiol* 61:51–59. doi:10.1016/j.yjmcc.2013.04.008
 16. Hale SL, Leeka JA, Kloner RA (2006) Improved left ventricular function and reduced necrosis after myocardial ischemia/reperfusion in rabbits treated with ranolazine, an inhibitor of the late sodium channel. *J Pharmacol Exp Ther* 318:418–423. doi:10.1124/jpet.106.103242
 17. Hamilton NB, Kolodziejczyk K, Kougioumtzidou E, Attwell D (2016) Proton-gated Ca²⁺-permeable TRP channels damage myelin in conditions mimicking ischaemia. *Nature* 529:523–527. doi:10.1038/nature16519
 18. Imahashi K, Pott C, Goldhaber JJ, Steenbergen C, Philipson KD, Murphy E (2005) Cardiac-specific ablation of the Na⁺–Ca²⁺ exchanger confers protection against ischemia/reperfusion injury. *Circ Res* 97:916–921. doi:10.1161/01.RES.0000187456.06162.cb
 19. Jung IS, Lee SH, Yang MK, Park JW, Yi KY, Yoo SE, Kwon SH, Chung HJ, Choi WS, Shin HS (2010) Cardioprotective effects of the novel Na⁺/H⁺ exchanger-1 inhibitor KR-32560 in a perfused rat heart model of global ischemia and reperfusion: involvement of the Akt-GSK-3 β cell survival pathway and antioxidant enzyme. *Arch Pharm Res* 33:1241–1251. doi:10.1007/s12272-010-0815-z
 20. Kaibara M, Kameyama M (1988) Inhibition of the calcium channel by intracellular protons in single ventricular myocytes of the guinea-pig. *J Physiol* 403:621–640. doi:10.1113/jphysiol.1988.sp017268
 21. Kirichok Y, Krapivinsky G, Clapham DE (2004) The mitochondrial calcium uniporter is a highly selective ion channel. *Nature* 427:360–364. doi:10.1038/nature02246
 22. Kohlhaas M, Maack C (2013) Calcium release microdomains and mitochondria. *Cardiovasc Res* 98:259–268. doi:10.1093/cvr/cvt032
 23. Lazdunski M, Frelin C, Vigne P (1985) The sodium/hydrogen exchange system in cardiac cells: its biochemical and pharmacological properties and its role in regulating internal concentrations of sodium and internal pH. *J Mol Cell Cardiol* 17:1029–1042. doi:10.1016/S0022-2828(85)80119-X
 24. Linz WJ, Busch AE (2003) NHE-1 inhibition: from protection during acute ischaemia/reperfusion to prevention/reversal of myocardial remodelling. *Naunyn Schmiedebergs Arch Pharmacol* 368:239–246. doi:10.1007/s00210-003-0808-2
 25. Lu J, Zang WJ, Yu XJ, Chen LN, Zhang CH, Jia B (2005) Effects of ischaemia-mimetic factors on isolated rat ventricular myocytes. *Exp Physiol* 90:497–505. doi:10.1113/expphysiol.2004.029421
 26. Ma J, Song Y, Shryock JC, Hu L, Wang W, Yan X, Zhang P, Belardinelli L (2014) Ranolazine attenuates hypoxia- and hydrogen peroxide-induced increases in sodium channel late openings in ventricular myocytes. *J Cardiovasc Pharmacol* 64:60–68. doi:10.1097/FJC.000000000000090
 27. Maack C, Cortassa S, Aon MA, Ganesan AN, Liu T, O'Rourke B (2006) Elevated cytosolic Na⁺ decreases mitochondrial Ca²⁺ uptake during excitation-contraction coupling and impairs energetic adaptation in cardiac myocytes. *Circ Res* 99:172–182. doi:10.1161/01.RES.0000232546.92777.05
 28. MacDonald AC, Howlett SE (2008) Differential effects of the sodium calcium exchange inhibitor, KB-R7943, on ischemia and reperfusion injury in isolated guinea pig ventricular myocytes. *Eur J Pharmacol* 580:214–223. doi:10.1016/j.ejphar.2007.10.055
 29. Matlib MA, Zhou Z, Knight S, Ahmed S, Choi KM, Krause-Bauer J, Phillips R, Altschuld R, Katsube Y, Sperelakis N, Bers DM (1998) Oxygen-bridged dinuclear ruthenium amine complex specifically inhibits Ca²⁺ uptake into mitochondria in vitro and in situ in single cardiac myocytes. *J Biol Chem* 273:10223–10231. doi:10.1074/jbc.273.17.10223
 30. Nakamura T, Hayashi H, Satoh H, Katoh H, Kaneko M, Terada H (1999) A single cell model of myocardial reperfusion injury: changes in intracellular Na⁺ and Ca²⁺ concentrations in guinea pig ventricular myocytes. *Mol Cell Biochem* 194:147–157. doi:10.1023/A:1006919929104
 31. Namekata I, Shimada H, Kawanishi T, Tanaka H, Shigenobu K (2006) Reduction by SEA0400 of myocardial ischemia-induced cytoplasmic and mitochondrial Ca²⁺ overload. *Eur J Pharmacol* 543:108–115. doi:10.1016/j.ejphar.2006.06.012

32. Park CO, Xiao XH, Allen DG (1999) Changes in intracellular Na^+ and pH in rat heart during ischemia: role of Na^+/H^+ exchanger. *Am J Physiol* 276:H1581–H1590
33. Robertson S, Thomson AL, Carter R, Stott HR, Shaw CA, Hadoke PW, Newby DE, Miller MR, Gray GA (2014) Pulmonary diesel particulate increases susceptibility to myocardial ischemia/reperfusion injury via activation of sensory TRPV1 and beta1 adrenoceptors. *Part Fibre Toxicol* 11:12. doi:[10.1186/1743-8977-11-12](https://doi.org/10.1186/1743-8977-11-12)
34. Rocchetti M, Sala L, Rizzetto R, Staszewsky LI, Alemanni M, Zambelli V, Russo I, Barile L, Cornaghi L, Altomare C, Ronchi C, Mostacciolo G, Lucchetti J, Gobbi M, Latini R, Zaza A (2014) Ranolazine prevents I_{NaL} enhancement and blunts myocardial remodelling in a model of pulmonary hypertension. *Cardiovasc Res* 104:37–48. doi:[10.1093/cvr/cvu188](https://doi.org/10.1093/cvr/cvu188)
35. Salameh A, Dhein S, Beuckelmann DJ (2002) Role of the cardiac Na^+/H^+ exchanger in $[\text{Ca}^{2+}]_i$ and $[\text{Na}^+]_i$ handling during intracellular acidosis. Effect of cariporide (Hoe 642). *Pharmacol Res* 45:35–41. doi:[10.1006/phrs.2001.0908](https://doi.org/10.1006/phrs.2001.0908)
36. Sanchez JA, Garcia MC, Sharma VK, Young KC, Matlib MA, Sheu SS (2001) Mitochondria regulate inactivation of L-type Ca^{2+} channels in rat heart. *J Physiol* 536:387–396. doi:[10.1111/j.1469-7793.2001.0387c.xd](https://doi.org/10.1111/j.1469-7793.2001.0387c.xd)
37. Saotome M, Katoh H, Satoh H, Nagasaka S, Yoshihara S, Terada H, Hayashi H (2005) Mitochondrial membrane potential modulates regulation of mitochondrial Ca^{2+} in rat ventricular myocytes. *Am J Physiol Heart Circ Physiol* 288:H1820–H1828. doi:[10.1152/ajpheart.00589.2004](https://doi.org/10.1152/ajpheart.00589.2004)
38. Sato R, Noma A, Kurachi Y, Irisawa H (1985) Effects of intracellular acidification on membrane currents in ventricular cells of the guinea pig. *Circ Res* 57:553–561. doi:[10.1161/01.res.57.4.553](https://doi.org/10.1161/01.res.57.4.553)
39. Soliman D, Wang L, Hamming KS, Yang W, Fatehi M, Carter CC, Clanachan AS, Light PE (2012) Late sodium current inhibition alone with ranolazine is sufficient to reduce ischemia- and cardiac glycoside-induced calcium overload and contractile dysfunction mediated by reverse-mode sodium/calcium exchange. *J Pharmacol Exp Ther* 343:325–332. doi:[10.1124/jpet.112.196949](https://doi.org/10.1124/jpet.112.196949)
40. Song Y, Shryock JC, Wagner S, Maier LS, Belardinelli L (2006) Blocking late sodium current reduces hydrogen peroxide-induced arrhythmogenic activity and contractile dysfunction. *J Pharmacol Exp Ther* 318:214–222. doi:[10.1124/jpet.106.101832](https://doi.org/10.1124/jpet.106.101832)
41. Swietach P, Youm JB, Saegusa N, Leem CH, Spitzer KW, Vaughan-Jones RD (2013) Coupled $\text{Ca}^{2+}/\text{H}^+$ transport by cytoplasmic buffers regulates local Ca^{2+} and H^+ ion signaling. *Proc Natl Acad Sci USA* 110:E2064–E2073. doi:[10.1073/pnas.1222433110](https://doi.org/10.1073/pnas.1222433110)
42. Tanaka H, Nishimaru K, Aikawa T, Hirayama W, Tanaka Y, Shigenobu K (2002) Effect of SEA0400, a novel inhibitor of sodium-calcium exchanger, on myocardial ionic currents. *Br J Pharmacol* 135:1096–1100. doi:[10.1038/sj.bjp.0704574](https://doi.org/10.1038/sj.bjp.0704574)
43. Tang Q, Ma J, Zhang P, Wan W, Kong L, Wu L (2012) Persistent sodium current and Na^+/H^+ exchange contributes to the augmentation of the reverse $\text{Na}^+/\text{Ca}^{2+}$ exchange during hypoxia or acute ischemia in ventricular myocytes. *Pflugers Arch* 463:513–522. doi:[10.1007/s00424-011-1070-y](https://doi.org/10.1007/s00424-011-1070-y)
44. Tanonaka K, Motegi K, Arino T, Marunouchi T, Takagi N, Takeo S (2012) Possible pathway of Na^+ flux into mitochondria in ischemic heart. *Biol Pharm Bull* 35:1661–1668. doi:[10.1248/bpb.b12-00010](https://doi.org/10.1248/bpb.b12-00010)
45. Undrovinas AI, Belardinelli L, Undrovinas NA, Sabbah HN (2006) Ranolazine improves abnormal repolarization and contraction in left ventricular myocytes of dogs with heart failure by inhibiting late sodium current. *J Cardiovasc Electrophysiol* 17(Suppl 1):S169–S177. doi:[10.1111/j.1540-8167.2006.00401.x](https://doi.org/10.1111/j.1540-8167.2006.00401.x)
46. Undrovinas AI, Fleidervish IA, Makielski JC (1992) Inward sodium current at resting potentials in single cardiac myocytes induced by the ischemic metabolite lysophosphatidylcholine. *Circ Res* 71:1231–1241. doi:[10.1161/01.res.71.5.1231](https://doi.org/10.1161/01.res.71.5.1231)
47. van Borren MM, Baartscheer A, Wilders R, Ravesloot JH (2004) NHE-1 and NBC during pseudo-ischemia/reperfusion in rabbit ventricular myocytes. *J Mol Cell Cardiol* 37:567–577. doi:[10.1016/j.yjmcc.2004.05.017](https://doi.org/10.1016/j.yjmcc.2004.05.017)
48. Wang XJ, Wang LL, Fu C, Zhang PH, Wu Y, Ma JH (2014) Ranolazine attenuates the enhanced reverse $\text{Na}^+/\text{Ca}^{2+}$ exchange current via inhibiting hypoxia-increased late sodium current in ventricular myocytes. *J Pharmacol Sci* 124:365–373. doi:[10.1254/jphs.13202FP](https://doi.org/10.1254/jphs.13202FP)
49. Wilde AA, Escande D, Schumacher CA, Thuringer D, Mestre M, Fiolet JW, Janse MJ (1990) Potassium accumulation in the globally ischemic mammalian heart. A role for the ATP-sensitive potassium channel. *Circ Res* 67:835–843. doi:[10.1161/01.res.67.4.835](https://doi.org/10.1161/01.res.67.4.835)
50. Williams IA, Xiao XH, Ju YK, Allen DG (2007) The rise of $[\text{Na}^+]_i$ during ischemia and reperfusion in the rat heart—underlying mechanisms. *Pflugers Arch* 454:903–912. doi:[10.1007/s00424-007-0241-3](https://doi.org/10.1007/s00424-007-0241-3)
51. Zaza A, Rocchetti M (2013) The late Na^+ current—origin and pathophysiological relevance. *Cardiovasc Drugs Ther* 27:61–68. doi:[10.1007/s10557-012-6430-0](https://doi.org/10.1007/s10557-012-6430-0)